



ANALYTICAL SERIES

Secondary Ion Mass Spectrometry of Automotive Coating Systems

by **Steven J. Simko, Steven L. Kaberline, and Larry P. Haack**
Ford Research and Innovation Center

This article is the final installment in a series focusing on surface analysis techniques. Previous articles examined x-ray photoelectron spectroscopy and Auger electron spectroscopy. These complementary methods serve as valuable tools for resolving questions on the surface composition of solid materials in applications such as automotive paint systems.

INTRODUCTION

Secondary ion mass spectrometry (SIMS) is a specialized form of surface analysis that is used primarily to determine the elemental and chemical structure of solid materials.^{1,2} It is based on mass spectrometry which is a family of techniques where elements, molecules, and molecular fragments are sorted based on their atomic/molecular weights. The technique employs a source to excite the material of interest into the gas phase with some portion of it as ionized species. The ions then pass through a mass filter which sorts them based on their mass-to-charge ratio. The resulting mass spectrum gives a representation of the elemental and/or molecular composition of the material of interest.^{1,3} Often, the list of molecular fragments in the spectrum can be pieced together to obtain a detailed understanding of the chemical structure of the material.^{1,3,4}

THEORY

In SIMS, the excitation source consists of a vacuum chamber and an ion gun. Placing the sample in a vacuum keeps the surface clean and allows for easy transport of ions through the instrument. The ion gun produces a stream of ions, called primary ions, that illuminate the sample. As the primary ions reach the sample surface, they transfer energy to the atoms in the solid through elastic collisions in a process called a “collision cascade.”⁵ A schematic diagram of this process is shown in *Figure 1*. Enough energy is transferred in the collision cascade to break chemical bonds and to displace atoms from their positions in the solid lattice. A small fraction of these atoms and molecular fragments obtain enough energy to escape the solid and enter the gas phase. Some of the ejected particles are electrically charged (ionized). These particles, called secondary ions, can be passed through a mass spectrometer to generate the SIMS spectrum of the solid.

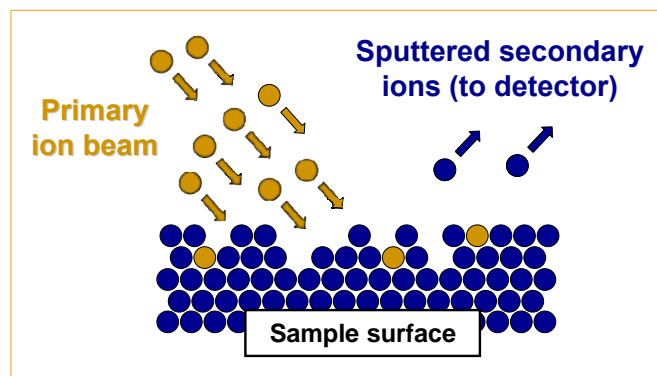


Figure 1—Simplified illustration of the ion sputtering process.

A number of different ion sources and mass spectrometers are available for performing SIMS experiments which gives the analyst great flexibility in designing how the experiment is performed. The experimental set-up also influences the type of data that can be generated. The wide variety of SIMS instrumentation can be classified into two general categories, dynamic SIMS and static SIMS.^{4,6} Historically, the first SIMS instruments that were developed were dynamic SIMS systems designed to take advantage of the method's high sensitivity which can approach parts-per-billion (PPB) levels.⁷ This is achieved in part by employing a high flux of primary ions. During analysis, a crater is eroded into the solid, producing enough secondary ions to achieve high sensitivity. These instruments have evolved into sophisticated systems designed to measure ultra low concentrations, depth distributions (depth profiles), and lateral distributions (maps) of elements.⁸ One of the main uses of dynamic SIMS is determining the distribution of dopants in semi-conductor devices. This information is indispensable in tailoring the electrical properties of a device and is responsible in part for the dramatic improvements in semi-conductor performance.³ However, the high primary ion fluxes employed in dynamic SIMS break most of the chemical bonds in the solid resulting in minimal structural and chemical information. Thus, dynamic SIMS has limited utility for studying coating systems which are often composed of organic materials.

This limitation was rectified in the late 1960s when Benninghoven introduced the concept of static SIMS.^{9,10} If the total flux of primary ions used in the experiment was held below a certain threshold, statistically each primary ion would interact with the solid in a region that was undamaged by a prior primary ion bombardment. Since these secondary ions had only suffered one collision cascade, they contain a higher percentage of molecular fragments that contain structural information about the materials in the solid. This threshold was dubbed the static limit ($<5 \times 10^{-12}$ ions/cm²), and the technique static SIMS.

Because the flux of secondary ions that are generated in static SIMS is so low, a mass spectrometer with high efficiency is desirable to maintain adequate sensitivity. The type of spectrometer that has proven most useful for the static SIMS experiment is the time-of-flight (ToF) mass spectrometer.¹ There are no signal-wasting slits in this spectrometer; instead, it relies on differences in flight time through the instrument to separate ions of different masses. Hence, a high percentage of the generated secondary ions is detected in this type of instrument. A schematic of the ToF spectrometer is shown in *Figure 2*. Note that the

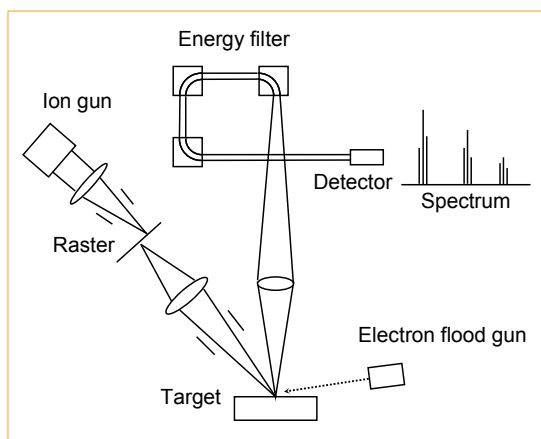


Figure 2—Schematic diagram of a ToF-SIMS spectrometer.

ion source generates a pulse of ions rather than a continuous stream. The arrival time of this primary ion pulse starts the time clock as this is the instant when secondary ions are generated. Secondary ions are accelerated to a constant kinetic energy using a grid held at a high electrical potential. They then pass through the long flight tube and hit the detector where the time clock is stopped. The arrival times of the secondary ions at the detector are determined by the simple kinetic energy equation:

$$KE = 1/2mV^2$$

where *KE* is the kinetic energy the ion receives from the acceleration grid, *m* is the mass of the ion, and *V* is the final velocity the ion.¹¹ If we substitute length of the flight tube (*d*) over flight time for velocity, this equation can be rearranged to:

$$flighttime = d / \sqrt{\frac{2KE}{m}}$$

Hence, flight time is inversely proportional to the square root of the ions' mass. Light ions take a short time to reach the detector and heavier ions take longer. The number of ions of a given mass are counted, resulting in an intensity at that mass. The resulting spectrum consists of a plot of intensity of ions as a function of mass. The rich collection of peaks in the resulting spectrum is representative of the composition of the solid and how elements are combined. The ability of ToF-SIMS to measure molecular fragments with high sensitivity makes it a popular choice for studying coating systems.¹²

Table 1 lists some key characteristics of the ToF-SIMS experiment.¹ Both positive and negative ions can be examined with this instrument. This increases the sensitivity of the technique as some materials produce high amounts of positive ions while others produce greater amounts of negative ions. The collision cascade only propagates a few monolayers into the solid so the technique is very

Table 1—Key Characteristics of the ToF-SIMS Experiment

ToF-SIMS Feature	Specification
Surface probe	Ion beam
Species detected	+/- ions
Analysis depth	Monolayers
Surface damage	Minimal
Detection limit	1 ppm
Spatial resolution	150 nm
Mass resolution	9,000
Analysis area	1 or 50 mm ²
Elements detected	All + isotopes
Quantification	Difficult
Molecular information	Fragments <= 20K amu

surface sensitive. Operating in the static regime results in minimal surface damage, yet SIMS can be very sensitive with detection limits in the 1 ppm range. The primary ion beam can be focused to a small diameter resulting in a spatial resolution of 150 nm. This allows characterization of small localized areas and/or generation of elemental and molecular fragment maps with high spatial detail. In addition, modern instruments have a movable stage which allows for examination of relatively large areas (up to 50 mm²).

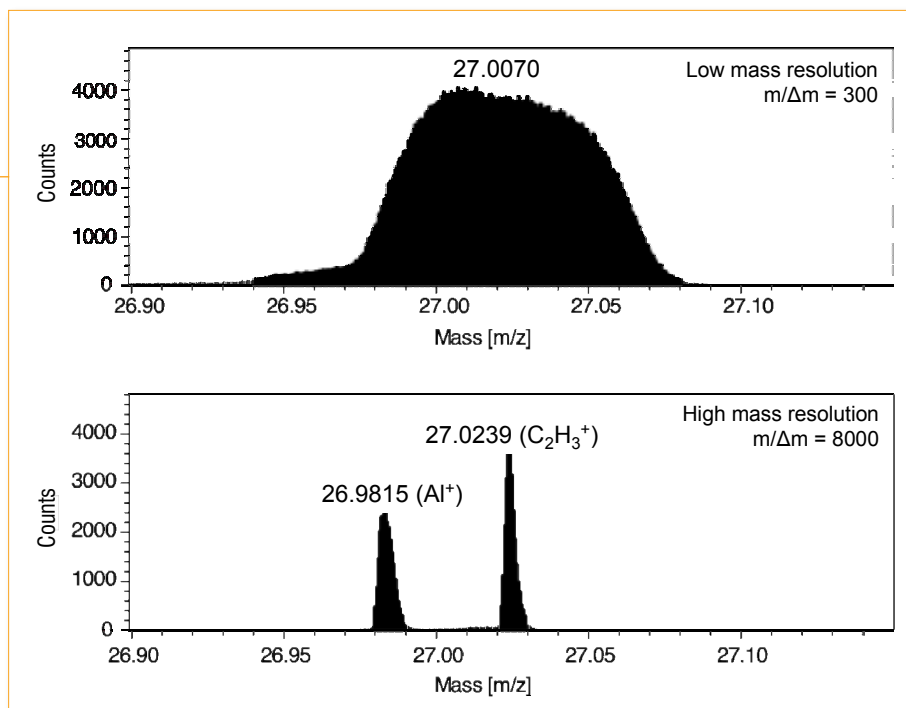
A great advantage of a ToF-SIMS instrument is that sample charging during analysis is not usually

a serious problem, even when dealing with non-conducting samples such as paints and polymers. There are two reasons for this. First, since the primary ion source is pulsed, the duty cycle of the primary ions is very low. Typically, the primary ion beam is “on” for only nanoseconds each pulse, then the electronics “wait” for milliseconds for all of the ions to reach the detector and be counted. Secondly, during this dead time while waiting for the ions to reach the detector, an electron flood gun can be used to direct a pulse of electrons onto the sample surface, which balances out the positive primary ions and greatly minimizes any sample charging.

Often ions of different elemental compositions will have the same nominal mass. This is illustrated in the comparison of low and high mass resolution spectra included in *Figure 3*. In this example, both aluminum (Al⁺) and the hydrocarbon fragment C₂H₃⁺ are present. The low mass resolution spectrum, m/Δm = 300, shows only a broad featureless peak at mass 27. However, the high mass resolution spectra at m/Δm = 8000 reveals two peaks separated by approximately 0.04 amu. Thus, the true masses of these two materials differ enough to allow for their peaks to be separated by operating the spectrometer at high mass resolution. In this example, the broad peak observed at mass 27 is actually composed of both aluminum (mass 26.9815) and the C₂H₃⁺ hydrocarbon fragment at mass 27.0239.

With SIMS analysis, all elements in the periodic table are detectable including hydrogen, which is a significant advantage over other surface analysis techniques. In addition, SIMS can identify differ-

Figure 3—Comparison of low mass resolution (top) and high mass resolution (bottom) SIMS spectra of the mass 27 region of a coating specimen.



ent isotopes of a given element which allows for interesting and powerful labeling experiments. Quantification is difficult as concentrations rely on the ionization efficiency of the elements and fragments, a parameter that can vary by several orders of magnitude. However, with effort and the use of suitable SIMS standards, quantitation of 10–20% is possible.

ANALYSIS METHODS

There is a lot of flexibility in how the SIMS instrument can be operated, which allows the analyst to tailor the experiment to the type of information that is needed. The simplest SIMS experiment is to obtain a spectrum from an area of interest on the surface of a material. Results are often compared to spectra obtained from the surrounding area and/or other samples. For example, *Figure 4* shows two SIMS spectra obtained from an automotive paint system where the clearcoat does not completely wet out on the basecoat, causing a crater to form. The spectrum from outside the crater (*Figure 4*, bottom) shows spectral peaks that can be attributed to the clearcoat paint system. In contrast, the spectrum from inside the crater (*Figure 4*, top) exhibits numerous peaks that can be identified as mass fragments from polydimethylsiloxane (PDMS). Siloxanes are common contaminants that possess low surface energy. The presence of a low-surface-energy contaminant will result in poor wetting of the subsequently applied paint layers. Only a few monolayers of PDMS will cause craters to form, so a surface sensitive analysis method such as SIMS is required to identify the presence of this material.

SIMS can also be used to generate chemical and elemental maps showing how elements and compounds are distributed laterally across the surface of a sample. This is accomplished by rastering the primary ion beam over the area of interest and tuning the mass spectrometer to pass only the selected masses of interest. Specific locations on the specimen where the material of interest is present result in a high SIMS signal when the beam is probing that location. The high signal is turned into a bright pixel on the SIMS map. The result is illustrated in *Figure 5* which is a SIMS map of the PDMS fragment (mass 73) from one of the paint craters previously discussed. For comparison, the figure also contains an optical micrograph of the paint crater showing the one-to-one correspondence between the crater and the PDMS contaminant on this coating surface. The high SIMS signal is present throughout the crater bottom showing that the contaminant is uniformly distributed in this area. This result confirms that PDMS contamination was the root cause of poor clearcoat wetting and crater formation.

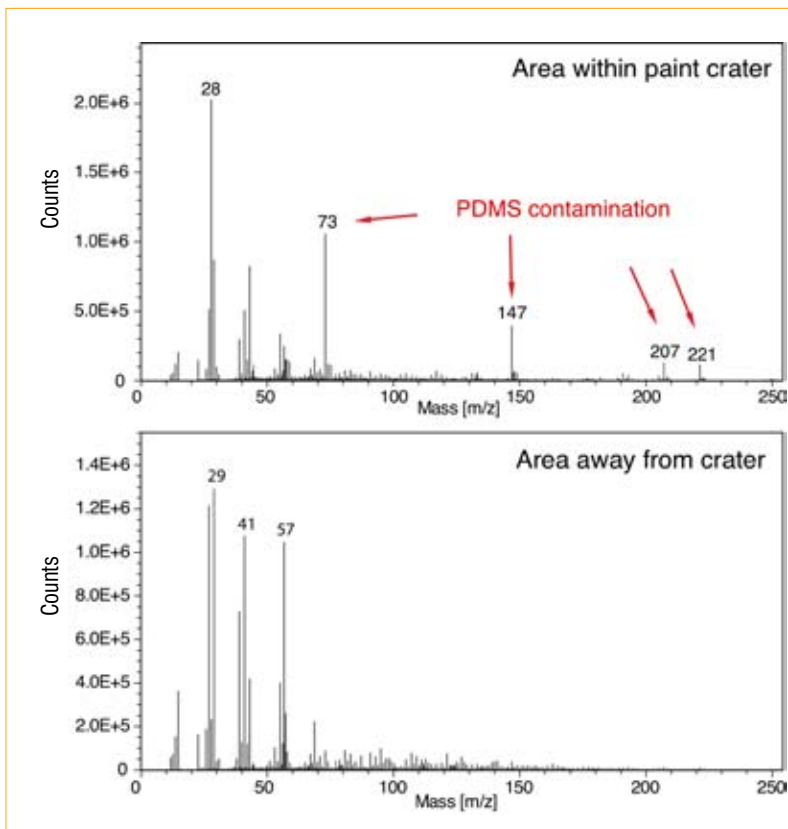


Figure 4—SIMS spectra of an automotive clearcoat specimen in a region with a crater defect (top) and a region with no crater defects (bottom).

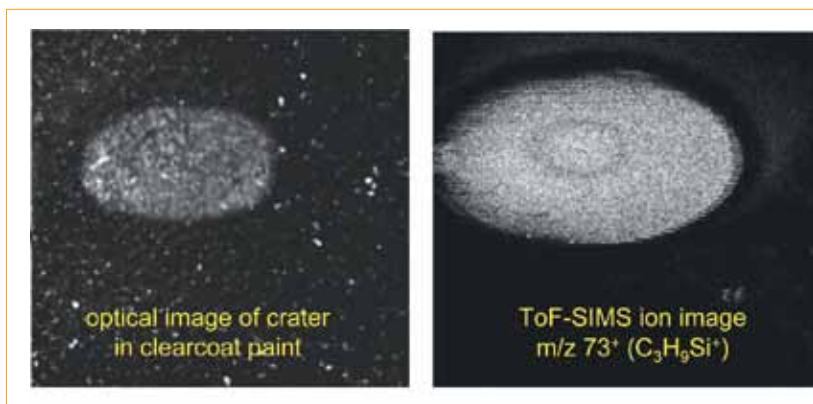


Figure 5—An optical micrograph of a crater defect in an automotive clearcoat specimen (left image) and a SIMS map of the mass 73 silicon-containing fragment from the crater.

The collision cascade that is the basis for SIMS results in material being removed from the sample surface during the experiment. When a high flux of primary ions is employed, this results in erosion of a crater into the specimen. Measuring the intensity of elements that are ejected from the sample as a function of sputter time results in a depth profile of the near surface region. The depth profile is useful for identifying how a solid might change in elemental composition from the top surface down into the

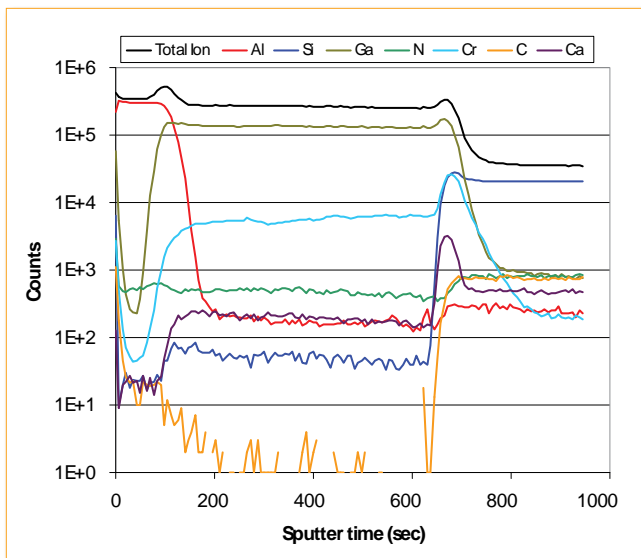


Figure 6—A SIMS sputter depth profile from a semi-conductor device specimen.

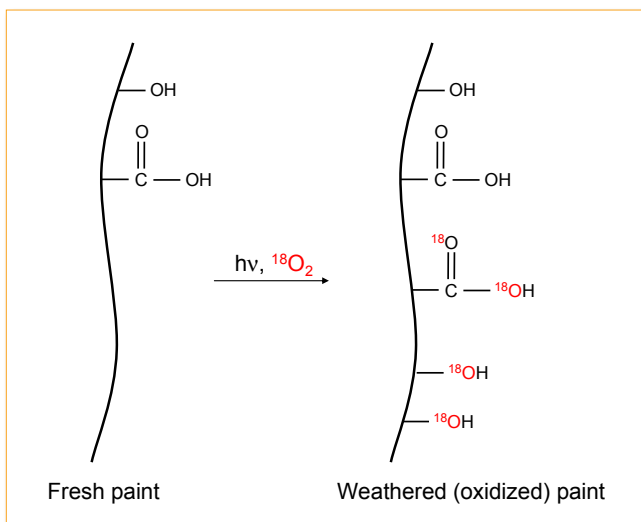


Figure 7—A schematic representation of a paint weathering experiment showing how photooxidation products get labeled with oxygen-18.

bulk of the material. An example of a SIMS depth profile is shown in *Figure 6*. The sample is a semi-conductor device with an aluminum surface film on top of a gallium-chromium layer on a silicon nitride substrate. The elemental composition of each layer and the contaminants that are distributed within each can be observed on this plot. However, limited chemical or molecular information about the sample is presented in the profile due to the extensive damage caused by the impact of the primary ion beam. Thus, analogous to dynamic SIMS mentioned earlier, damage caused by extended exposure of the primary ion beam in sputter depth profiling also limits the utility of this technique for determining molecular or structural information as a function of depth in organic coating systems.

The high sensitivity of SIMS is an important advantage over other surface sensitive analysis techniques which allows the experiment to be conducted in unique ways. For example, elemental mapping can be combined with sputter depth profiling to generate a three-dimensional image of the specimen. These images show the distributions of elements both laterally across the surface as well as a short depth into the specimen. The utility of generating three-dimensional maps will be demonstrated in the following Applications section by revealing how bake ovens can alter the surface chemistry of organic coatings during the cure process.

APPLICATIONS OF SIMS TO PAINT TECHNOLOGY

The ability to analyze insulating samples with high sensitivity and high spatial resolution makes SIMS an ideal method for characterizing paint and coating systems. In the Ford Research Lab, SIMS is routinely used to study and compare the extent of paint weathering and how stabilizing additives are distributed within the coating system. A few examples of these studies are highlighted as follows.

When a paint system is exposed to UV light or sunlight in an oxygen atmosphere, photooxidation occurs.^{13,14} Bonds are broken and atmospheric oxygen reacts with paint molecules to produce carboxylic acids, alcohols, ketones, and other oxidized species. Because there already are significant amounts of oxygen incorporated in the paint system molecules (approximately 15% atomic), it is impossible to measure the photooxidation products directly with SIMS as any oxygen-containing fragments could be the result of either undisturbed paint molecules or photooxidation. However, by taking advantage of the ability of SIMS to separate and measure isotopes, the photooxidation products can be labeled with a unique isotope of oxygen, allowing direct measurement of the photooxidation products (see *Figure 7*).^{15,16} If the paint system is exposed to UV light in an atmosphere of oxygen-18, then oxygen-18 labeled photooxidation products will be created.

Figure 8 outlines the oxygen labeling experiment. A complete automotive paint system (clearcoat/basecoat/primer/electrocoat) is sealed in an air-tight chamber fitted with a quartz UV-transparent window. The chamber is evacuated and back-filled with a (3:1) mixture of oxygen-18 gas and nitrogen. The paint system is exposed top-down (i.e., through the clearcoat) to UV light. Depending on the reactivity of the paint system, oxygen-18 can permeate into subsurface regions and possibly react with the different coating layers through photooxidation. After exposure, the paint sample is microtomed edge-on to produce a

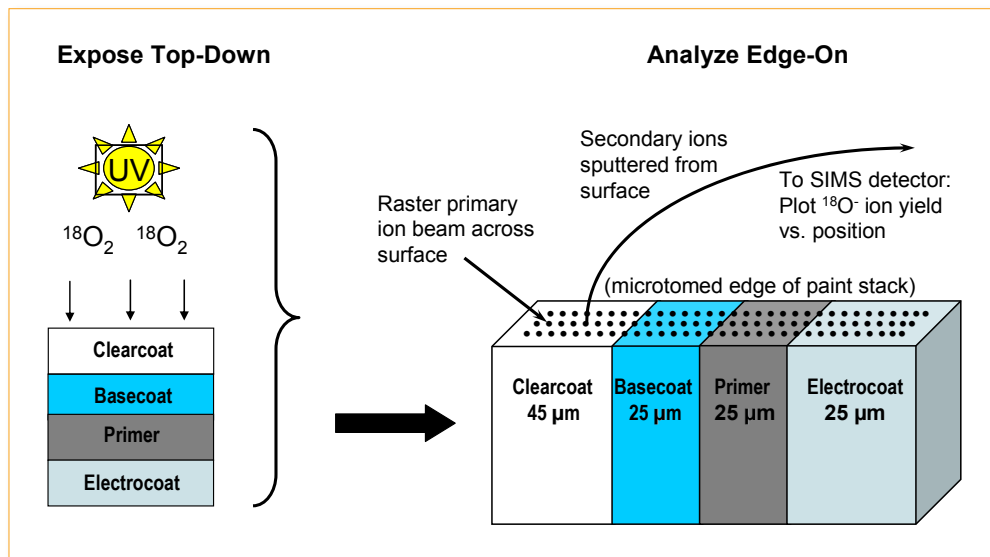


Figure 8—A schematic representation of the oxygen-18 weathering experiment showing the specimen orientation during light exposure (left) and analysis (right).

smooth cross-section allowing examination of all the paint layers by SIMS. During SIMS analysis, the primary ion beam is rastered across this smooth cross-section and the resulting secondary ions are detected. The photooxidation products are readily detected with SIMS by analyzing fragments that have unique masses due to the presence of the oxygen-18 isotope. Elemental and chemical fragment maps can be generated to reveal where photooxidation has occurred within the stack of layers forming the automotive paint system.

The use of high-intensity artificial sunlight combined with the sensitivity of the SIMS allows for very short UV exposure times. This greatly accelerates the photooxidation process allowing coating systems to be evaluated in much less time than with conventional weathering tests. Several weeks of exposure in the oxygen-18 cell can produce photooxidation results that are equivalent to several years of exposure in Florida-based weathering experiments. These experiments have been shown to provide critical information to paint design engineers as they can be used to rapidly predict the weathering durability of paint formulations in development for future paint systems.

Figure 9 shows the results of a typical oxygen-18 weathering experiment. On the left side is the oxygen-18 map showing the locations where photooxidation had occurred. On the right side is a corresponding oxygen-18 linescan which was generated by drawing a vertical line from the top of the map through to the bottom and then plotting the pixel count value at each linescan point. The oxygen-18 signal associated with the reactivity of each layer within the paint system can be readily identified. The two layers marked “std” are an

oxygen-18 reference standard that is sandwiched over the sample before microtoming. They serve as markers to delineate the location of the coating layers and to calibrate the intensity of the oxygen-18 signal. On the top of the clearcoat layer, a thin layer of surface oxidation is apparent. This thin layer is typically seen on the top clearcoat surface of all exposed paint systems and corresponds to the small amount of photooxidation that occurs on the unprotected paint surface. The remainder of the clearcoat layer shows only a small amount of photooxidation.

In this example, the top surface of the basecoat also shows a small amount of photooxidation indicated by the rise in the oxygen-18 signal at the surface of this layer. For the basecoat, this indicates that the light absorbing additives (UVA additives) in the clearcoat are not completely

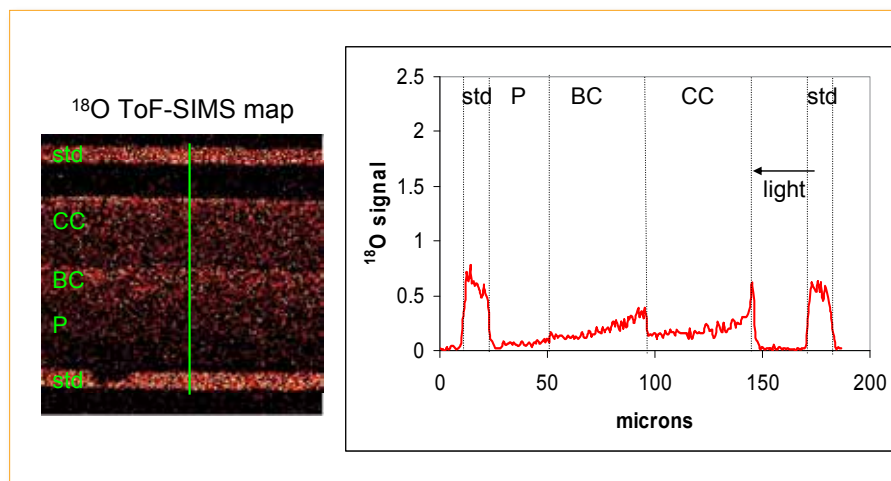


Figure 9—Oxygen-18 weathering results from a paint system that exhibits acceptable performance. The SIMS map for mass 18 (O-18) is shown at left and the corresponding linescan displaying relative intensities in the different paint regions is shown on the right. Std=standard, P=primer, BC=basecoat, CC=clearcoat.

Figure 10—Oxygen-18 weathering results from a paint system that exhibits poor performance. The SIMS map for mass 18 (O-18) is shown at left and the linescan showing relative intensities of oxygen-18 in the different paint regions is given on the right. Std=standard, P=primer, BC=basecoat, CC=clearcoat.

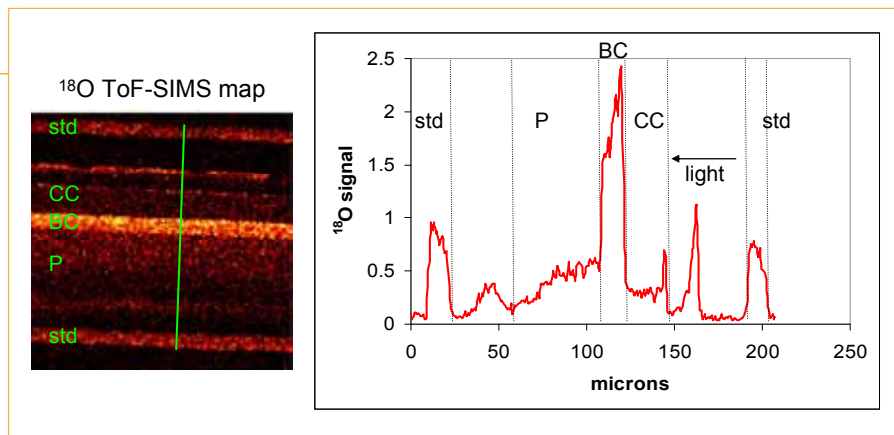


Figure 11—Oxygen-18 weathering results from a paint system showing the difference in weathering performance for three different colors. The SIMS map for mass 18 (O-18) from the white paint is shown at left and the linescan showing relative intensities in the different paint regions for all three colors tested is shown on the right. Std=standard, P=primer, BC=basecoat, CC=clearcoat.

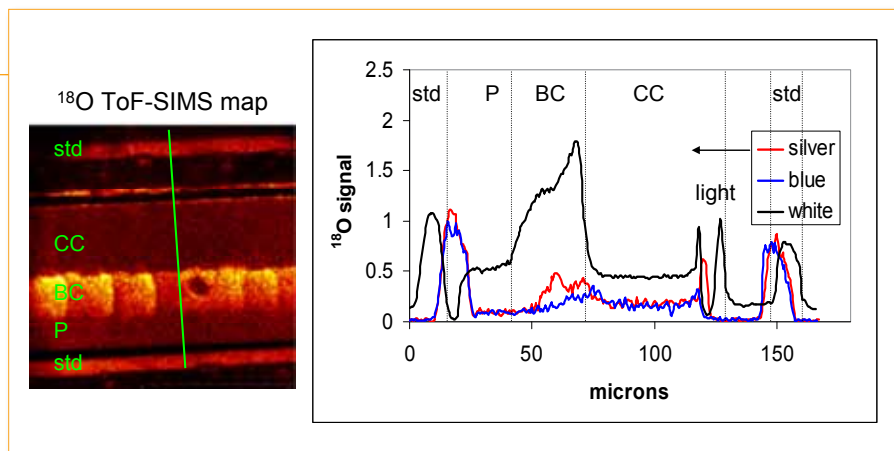
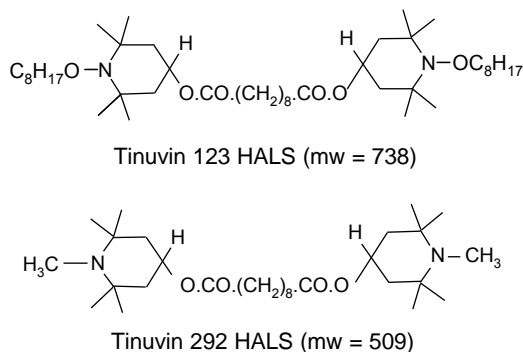


Figure 12—Structural representations of two common hindered amine light stabilizer additives.



effective at blocking all of the light and photooxidation of the basecoat top surface is beginning to occur. There is no oxygen-18 signal in the primer. Thus, for this paint system, the UVA additives in the clearcoat along with the pigment in the basecoat are effectively blocking all light from the primer. This sample was exposed for only 200 hr (eight days) in the oxygen-18 cell which equates to three months' Florida exposure. Even from this short exposure time, the overall longevity of this paint system can be predicted to be "good."

Figure 10 shows the weathering results obtained from a different paint system. In this exam-

ple, we see not only the typical thin layer of surface oxidation in the clearcoat, but also a strong signal for oxygen-18 in the basecoat. There is concern about the long-term durability of this paint, and it can be predicted that the system will eventually fail by cracking and peeling with adhesion loss at the basecoat layer. This is an example of a paint system which is predicted to fail prematurely in service.

An experiment designed to rapidly compare the UV performance of multiple paint systems is shown in Figure 11. These paint systems were identical except for the color of the basecoat layer, which was either silver, blue, or white. The UV exposures and the sample preparation methods were also identical. Figure 11 shows the oxygen-18 map generated from the paint system with the white basecoat layer. The graph shows the SIMS linescans from all three paint systems superimposed onto one plot.

The results reveal clear differences in photooxidation susceptibility of the three colors. Under the same UV exposure conditions, the white color basecoat shows much more photooxidation than either the silver or blue colors. Based on these results, the white paint system was reformulated to bring its photooxidation performance to the same level as the other colors that were tested.

This example illustrates how the oxygen-18 ToF-SIMS technique offers a rapid way to compare the weathering performance of “identical” coating systems. The SIMS allows one to quickly identify minor differences in weathering that would not be easy to accomplish by any other analytical technique.

Much of the weathering performance of the paint systems included in the examples is governed by the additives that are incorporated into each layer to absorb light photons and prevent them from generating photooxidation reactions. Two important classes of these compounds are long wavelength (400–320 nm) ultraviolet light absorbers (UVAs) and hindered amine light stabilizers (HALS), which are effective at preventing photooxidation reactions when incorporated into coatings at low concentrations, typically 1–2%. The low concentration levels present a challenge for analyzing their presence and location within the coating system. However, the sensitivity and microanalysis capability of SIMS makes it an ideal technique for studying these coating additives.

The chemical formula and structure of two commonly used HALS additives, Tinuvin 123 (mw 738) and Tinuvin 292 (mw 509), are given in *Figure 12*. Despite their low concentration, these additives can yield a strong SIMS signal and can be readily detected. *Figure 13* includes three spectra that illustrate how SIMS can identify the presence of the Tinuvin 123 (mw 738) additive within a paint system. The top mass spectrum in *Figure 13* shows the high mass portion of the mass spectrum from the surface of an automotive clearcoat containing no additives. The hydrocarbon peaks present at nearly every mass are from the clearcoat chemistry as well as from an adventitious carbon contamination layer on the surface. There are no additive peaks detected in this spectrum. The bottom spectrum contains the mass spectrum of a sample of pure liquid Tinuvin 123 acquired from a one-nanoliter droplet deposited on a clean silicon wafer. The clearcoat system shown in the middle spectrum contained a 2% Tinuvin 123 additive. Note that the SIMS data in this mass region is nearly identical to the pure Tinuvin 123 standard. From this data it was determined that the signal strength of the mass 608 peak of Tinuvin 123 in the clearcoat is strong enough to identify as little as 0.2 wt% of the additive in the paint system.

The high sensitivity of ToF-SIMS allows the mapping of these additives in order to track migration and longevity. An experiment was conducted in which a three-layer clearcoat test sample was generated, containing 4%, 2%, and 1% concentrations of Tinuvin 292 light stabilizer. Each layer was completely cured before the next layer was added to the stack. SIMS data were acquired immediately

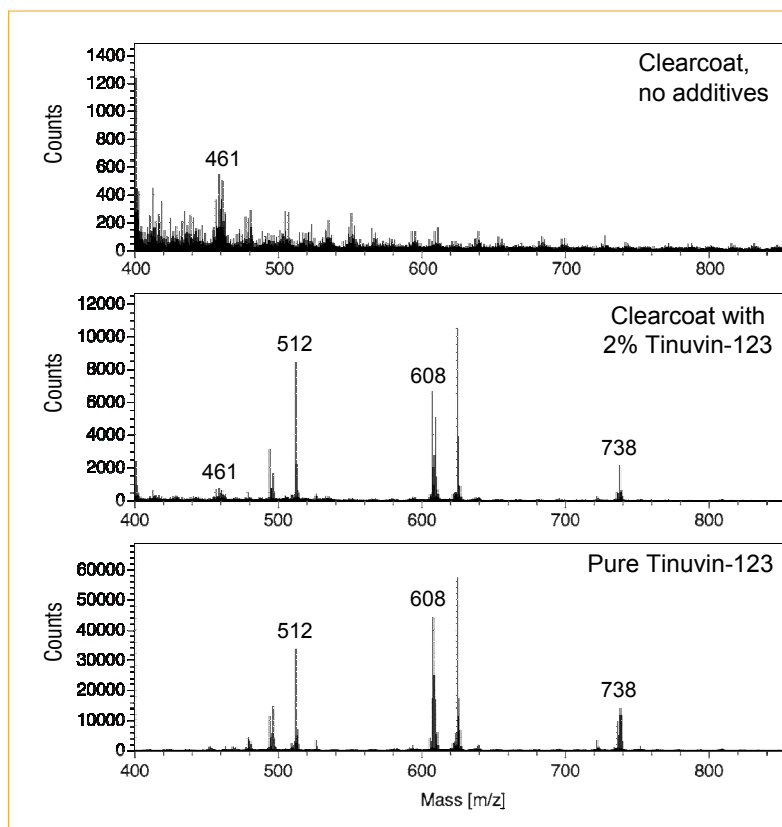


Figure 13—SIMS spectra from an automotive clearcoat with no additives (top), a HALS additive (bottom), and a clearcoat containing 2% of the HALS additive (middle).

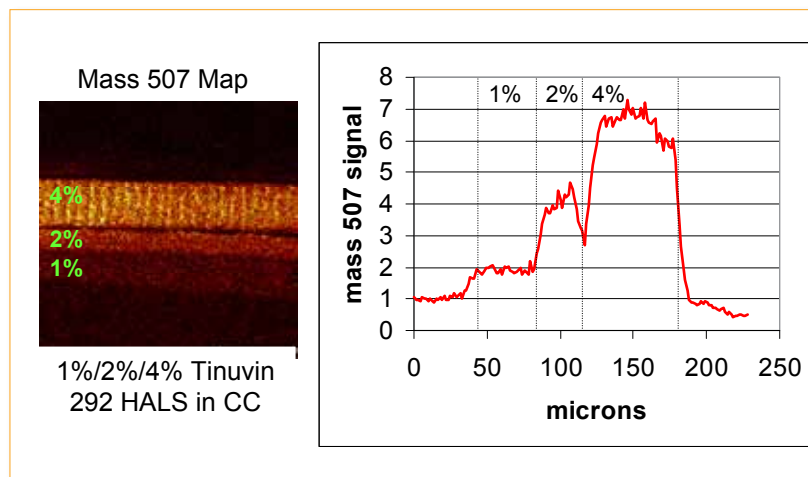


Figure 14—SIMS data from a paint stack constructed with three automotive clearcoat specimens that contain different amounts of the HALS, Tinuvin 292, after one week of aging. The SIMS map for mass 507 is shown at left and a line scan through the map showing the relative intensity changes is shown on the right.

after this paint stack was constructed and again after one week of aging at room temperature in a laboratory environment. The peak at mass 507 was used to characterize the additive as it tracks one of the unique molecular ions for Tinuvin 292. The paint stack was microtomed edge on and then analyzed by ToF-SIMS. The results after one week of aging are shown in *Figure 14*. The three distinct Tinuvin

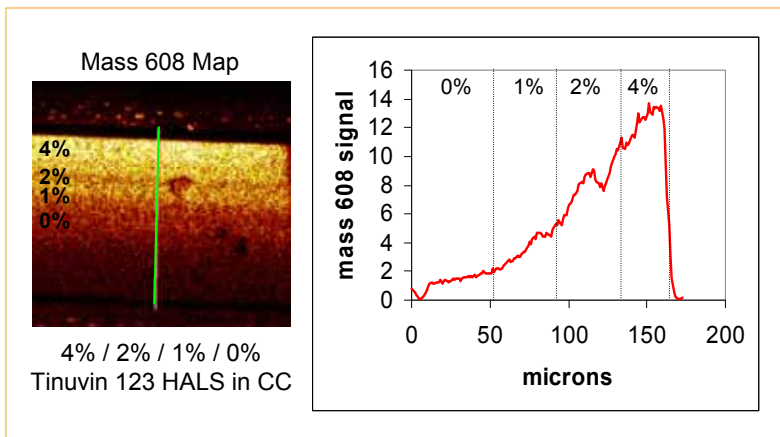


Figure 15—SIMS data from a paint stack constructed with four automotive clearcoat specimens that contain different amounts of the HALS, Tinuvin 123. The SIMS map for mass 608 is shown at left and a line scan through the map showing the relative intensity changes is shown on the right.

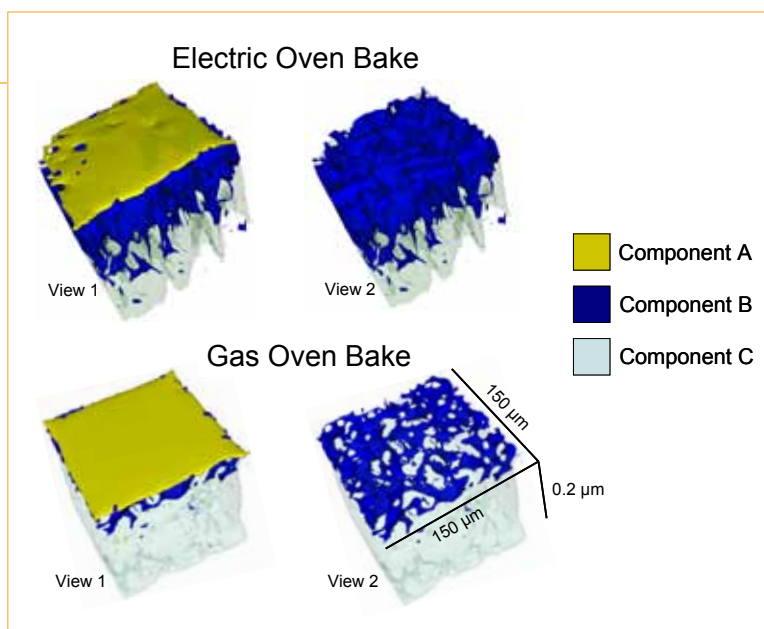
layers are still intact and show minimal diffusion when compared to the unaged sample (not shown).

The same experiment was repeated, this time using a different HALS additive, Tinuvin 123, and four layers containing 4%, 2%, 1%, and 0% concentrations of the light stabilizer. The Tinuvin 123 fragment peak at mw 608 was selected for mapping this compound as it was an intense peak in the spectrum and had no interfering contributions from clearcoat fragments (see *Figure 13*). The results from the freshly constructed paint stack (not shown) are similar to the Tinuvin 292 results discussed previously, with four distinct layers visible. However, in contrast to the Tinuvin 292 additive, the Tinuvin 123 shows extensive diffusion into adjacent layers after just one week of aging (see *Figure 15*). The signal profile exhibits a continuous gradient and the distinct layers are no longer

discernable. The linescan plot clearly shows the extent of the additive migration. It is remarkable that just a change in aliphatic end groups, or what might be considered a minor structural change in the Tinuvin molecule (see the chemical compositions in *Figure 12*), has such a large effect on the diffusion of the additive in the clearcoat. With this information, the Tinuvin additive can be tailored to the given application and designed to either enhance or retard its diffusion within a coating system.

A final example highlights how ToF-SIMS can be used to characterize chemistry induced in a paint coating during bake oven cure. It is known that water vapor and nitrogen oxides formed in the combustion exhaust of gas fired bake ovens can react with the surface of a coating during cure.^{17,18} For example, experiments revealed that nitrogen oxide radicals can react with and remove a crater-control additive from the surface of an epoxy-based electrocoat during cure. This chemistry did not occur when the epoxy was cured in an electric bake oven. In the example, the top clearcoat of an automotive paint system was cured either in an electric or gas fired oven in order to identify whether differences in surface chemistry would occur. These specimens were analyzed by ToF-SIMS three-dimensional depth profiling, which combines elemental mapping with sputter depth profiling to create a visual representation of where species exist within the near surface in the paint clearcoat. The three-dimensional maps in *Figure 16* show the distribution of three different components after either gas or electric oven cure. View 1 includes a map of components A, B, and C, while View 2 removes component A from the map allowing visualization of the layers beneath. It can be seen that Component A forms a thin, uniform coating on

Figure 16—Three-dimensional image depth profiles from automotive clearcoat specimens after baking in an electrical oven (top) or a gas-fired oven (bottom). View 1 contains data from three different components while View 2 is the same data with component A removed for easier viewing of the other two components.



both specimens. In contrast, component B forms a thick, uniform film on the panel baked in the electric oven but a thin, patchy layer on the panel baked in the gas-fired oven. This variation in the distribution of component B clarified why adhesion performance differences were observed on panels baked in the different cure ovens. Based on these results, recommendations were made to specify the precise paint formulation to employ based on the type of bake oven used to cure the coating.


CONCLUSIONS

Previous articles in this journal^{19,20} have shown that x-ray photoelectron spectroscopy (XPS) and Auger electron spectroscopy (AES) can be useful surface analysis tools for characterizing materials and coatings. XPS is excellent for accurately determining the composition and chemical state of elements, while AES excels in measuring the integrity of conversion layers used to impede corrosion on metal substrates under coatings.

The great flexibility of ToF-SIMS completes this suite of surface analysis techniques. ToF-SIMS complements XPS and AES with the ability to yield molecular information with high sensitivity at high spatial resolution. The rich structural information provided by SIMS is unique in a surface analysis technique, and the wide variety of experiments that are available make SIMS the ideal analysis method for studying a variety of coatings issues.

In automotive paint systems the technique can serve as a problem-solving tool to elucidate the presence of contaminants, while at the same time serve as a premier research tool that can measure and quantify the migration of additives. Its ability to measure isotopes allows the analyst to perform interesting and powerful labeling experiments that can predict the longevity of coating systems. In the future, ToF-SIMS will serve well as an analysis tool and as a predictive tool to help design and formulate the next generation of coatings for a wide variety of industries and applications.

ACKNOWLEDGMENT

The authors thank Ann Straccia for assistance in gathering ToF-SIMS data for the figures. 

References

1. Benninghoven, A., Rudenauer, F.G., and Werner, H.W., *Secondary Ion Mass Spectrometry*, John Wiley & Sons, New York, NY, 1987.
2. *Methods of Surface Analysis*, A.W. Czanderna (Ed.), Elsevier Sci. Pub. Co., New York, NY 1975.
3. Seah, M.P. and Briggs, D., *Practical Surface Analysis Volume 2—Ion and Neutral Spectroscopy*, 2nd edition, John Wiley & Sons, Chichester, UK, 1992.

4. Colton, R.J., "Molecular Secondary Ion Mass Spectrometry (SIMS)," *J. Vac. Sci. Technol.*, 18 (3), 737-747 (1981).
5. Winograd, N. and Garrison, B.J., "Surface Structure Determinations with Ion Beams," *Acc. Chem. Res.*, 13, 406-412 (1980).
6. Newman, J.G., Carlson, B.A., Michael, R.S., Moulder, J.F., and Hohlt, T.A., *Static SIMS Handbook of Polymer Analysis*, Physical Electronics Inc., Eden Prairie, MN, 1991.
7. Honig, R.E., "The Growth of Secondary Ion Mass Spectrometry (SIMS): A Personal View of Its Development," in *SIMS V*, Benninghoven, A., Colton, R.J., Simons, D.S., and Werner, H.W. (Eds.), Springer-Verlag, Berlin, Germany 1986.
8. de Chambost, E., Merkulov, A., Peres, P., Rasser, B., and Schuhmacher, M., "Latest Developments for the Cameca ULE-SIMS Instruments: IMS-Wf and SC-Ultra," *Applied Surface Sci.*, 231-232, 949-953 (2004).
9. Benninghoven, A., "The Analysis of Monomolecular Layers of Solids by Secondary Ion Emission," *Z. Physik*, 230, 403-413 (1970).
10. Benninghoven, A., "Observing Surface Oxidation of Molybdenum with the Static Method of Secondary Ion Mass Spectrometry," *Chem. Phys. Letters*, 6, 616 (1970).
11. Cotter, R.J., "Time-of-Flight Mass Spectrometry: Instrumentation and Applications in Biological Research," American Chemical Society, Washington, DC, 1997.
12. Brenda, M., Doring, R., and Schernau, U., "Investigation of Organic Coatings and Coating Defects with the Help of Time-of-Flight Secondary Ion Mass Spectrometry," *Prog. Org. Coat.*, 35, 183-189 (1999).
13. Wypych, G., *Handbook of Material Weathering*, 2nd Ed., Chem. Tec. Publishing, Ontario, Canada 1995.
14. Hamid, S.H., Amin, M.B., and Maadlan, A.G., *Handbook of Polymer Degradation*, Marcel Dekker, Inc., New York, NY, 1992.
15. Gerlock, J.L., Prater, T.J., Kaberline, S.L., and deVries, J.E., "Assessment of Relative Photooxidation Rates in Multi-Layer Coating Systems by Time-of-Flight Secondary Ion Mass Spectrometer," *Polym. Deg. & Stab.*, 47, 405 (1995).
16. Gerlock, J.L., Prater, T.J., Kaberline, S.L., Dupuie, J.L., Blais, E.J., and Rardon, D.E., "¹⁸O-Time-of-Flight Secondary Ion Mass Spectrometry Technique to Map the Relative Photooxidation Resistance of Automotive Paint Systems," *Polym. Deg. & Stab.*, 65, 37 (1999).
17. Haack, L.P. and Holubka J.W., "Bake Oven Induced Variation of Surface Chemistry on Electrocoat Paint: Effect on Primer-Electrocoat Intercoat Adhesion," *J. Coat. Technol.*, 72 (903), 63 (2000).
18. Haack L.P. and Holubka J.W., "Influence of Coating Formulation Variables and Processing on the Adhesion of Melamine-Crosslinked Polyester Primer to Urethane-Crosslinked Epoxy Electrocoat," *J. Coat. Technol.*, 72 (905), 61 (2000)
19. Haack, L., "X-ray Photoelectron Spectroscopy as an Analysis Tool for Coatings," *JCT CoatingsTech*, 8 (2) 42-51 (2011).
20. Simko, S.J., "Auger Electron Spectroscopy (AES) and Sputter Depth Profiling for Characterization of Metal Substrates and Pretreatment Coatings," *JCT CoatingsTech*, 8 (3) 52-58 (2011).

AUTHORS

Steven J. Simko, Steven L. Kaberline, and Larry P. Haack, Ford Research and Innovation Center, 2101 Village Rd., Dearborn, MI 48121; ssmiko@ford.com.